UDC: 528.8

E. O. ORYNBASSAROVA[1], *Head of the Department, Associate Professor, e.orynbassarova@satbayev.university*
B. ADEBIYET[1], *PhD Student*
F. A. ILIUF[1], *Student, Master of Engineering Sciences*
N. K. SYDYK[2], *Head of Laboratory, Candidate for a Doctor's Degree*

[1]*Satbayev University, Almaty, Kazahstan*
[2]*Institute of Ionosphere LLP, Almaty, Kazahstan*

ANALYSIS OF MINERAL INDICES FROM REMOTE SENSING: A CASE-STUDY OF THE TOKRAU RIVER

The study focuses on the use of the Earth Remote Sensing (ERS) data to calculate mineral indices using the example of the Tokrau River. In the modern era, as issues of climate change and human impact on the environment become increasingly prominent, monitoring natural resources has become imperative. In this regard, remote sensing technologies provide valuable data for the study and control of Earth's resources.

The aim of this research is to investigate changes in the mineral composition in the Tokrau River valley using information obtained during Landsat and Sentinel-2A missions from 1998 to 2021 to assess human impact on the ecosystem and to find potential mineral deposits.

This work is important both scientifically and practically as it demonstrates that spectral mapping can effectively detect mineral changes. This finding is significant for geological research and environmental monitoring.

The research approach included the examination of satellite data, calculation of mineral indices, and comparison of the results obtained in different time periods. The collected data allowed for conclusions to be drawn regarding fluctuations in mineral transformations in the Tokrau River valley.

The study complements existing knowledge about the use of remote sensing in geological research and environmental monitoring. It also contributes to international experience in this field. The practical significance of the research lies in utilizing the collected data to develop methods for the protection and responsible use of natural resources in the Tokrau River region and other comparable regions.

Keywords: *Earth remote sensing (ERS), mineral indices, Tokrau River, spectral analysis, Landsat, Sentinel-2A*
DOI: *10.17580/em.2024.01.17*

Introduction

In our time, as climate change and human impact on the environment become increasingly noticeable, it is critically important to monitor natural resources. In light of these challenges, remote sensing technologies (RS) acquire special significance for the study of Earth's resources, providing valuable information for their management.

Monitoring mineral indices plays a key role, allowing us to understand the geological history of regions and assess the human impact on the environment. Such an approach contributes to the development of strategies for the preservation and sustainable use of natural resources.

In the context of Kazakhstan, where the search and exploration of new mineral deposits are essential tasks, the application of remote sensing (RS) becomes particularly significant. The use of satellite data enhances the precision of research, making it easier to identify geological structures and discover promising deposits.

International experience, including studies conducted in Nevada (USA) and Northern Chile, demonstrates the effectiveness of spectral mapping in detecting hydrothermal alterations and gold deposits applicable to various types of deposits, including copper porphyry and epithermal veins. In the state of Nevada (USA), spectral methods have shown the capability to map minerals and rocks containing ammonium [1].

One of the most common objects of study are copper porphyry deposits, which are characterized by regularly changing, contrastingly mineralogical zonation of hydrothermal alterations. Spectral mapping of porphyry deposits has been carried out in the Silver Belt region, Arizona, USA [2], Collahuasi, Northern Chile [3], and some others [4]. As a result of the research, propylitic, argillic and phyllitic zones of hydrothermal metasomatic alterations were identified in the host rocks.

Quartz-vein epithermal gold deposits were studied in the Goldfield Mining District, Nevada, USA [5]. K. Watson [6] utilized thermal infrared multispectral data (TIMS) to investigate Carlin-type gold deposits in the USA. Gold deposits of various genesis, including hydrothermal, skarn, epithermal vein, bonanza-type, granite, porphyritic mineralization and sedimentary types, were examined in the Santa Teresa District, Sonora, Mexico, using Landsat satellite data [7]. ASTER radiometer data were employed to identify altered rock formations in the Chocolate Mountains, California, USA, for the localization of gold occurrences within quartz–biotite gneisses and muscovite schists of the Precambrian basement. In a series of studies in Kazakhstan, research has been conducted on the geological features and dynamics of the Karsakpai–Ulytauskaya geosuture zone, as well as an assessment of the potential mineral resources of this area [8].

In this study, our focus is on the Tokrau River in Kazakhstan. Utilizing data from Landsat and Sentinel-2A missions spanning from 1998 to 2021, we are analyzing mineralogical changes in the river valley. The objective of this research is not only to provide new insights into the mineralogy of the region but also to contribute to the understanding of the global utilization of remote sensing in the fields of geology and environmental monitoring.

Study area

From an administrative perspective, the Tokrau River (**Fig. 1**) falls within the Aktogai District of the Karaganda Region in Kazakhstan. The northern boundary of Tokrau is defined by the settlement of Ak-Tumsuk. The study area is situated within specific coordinates, encompassing the Tokrau River valley, bounded by the following coordinates to the north: 47°06'01" N — 75°16'43" E and 47°06'11" N — 75°43'18" E, and to the south: 46°39'48" N — 75°00'28" E and 46°43'58" N — 75°41'19" E.

Fig. 1. The studied section of the Tokrau River

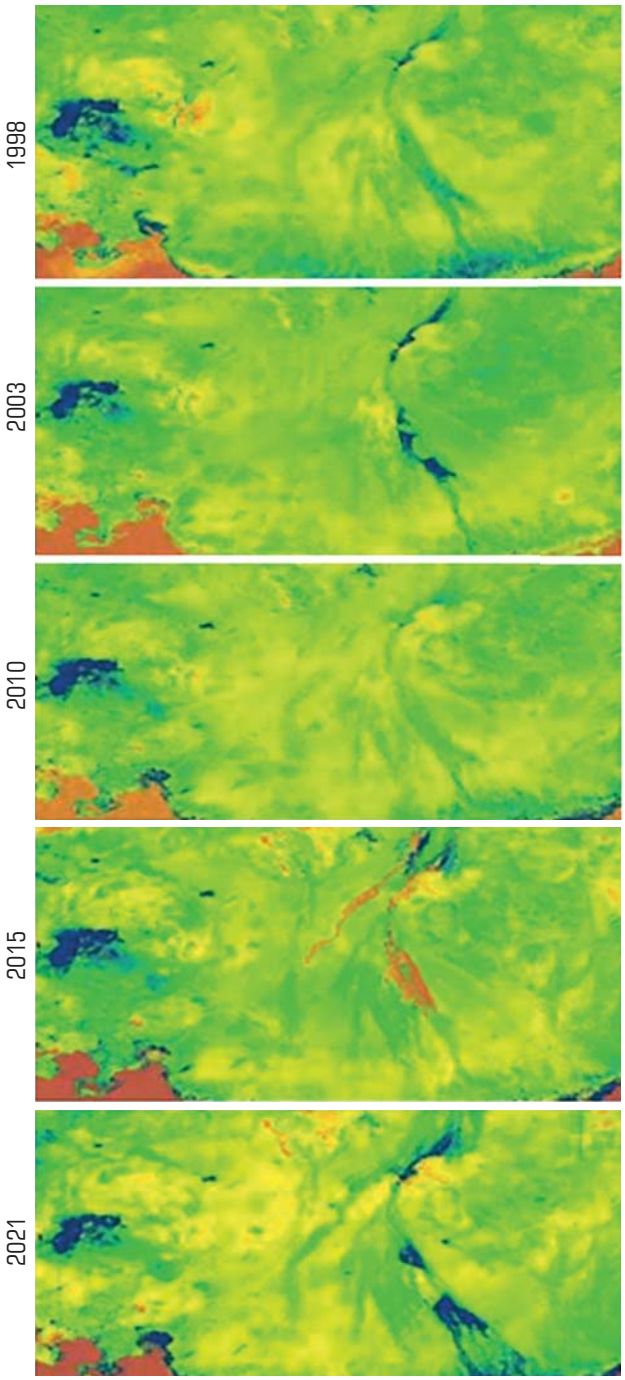

Fig. 2. Results for the Clay Minerals Index

The climate of the studied area is characterized by distinct continental features and aridity, typical of desert and semi-desert regions. This includes a wide range of temperature fluctuations, both on a monthly and daily basis, a low and uneven distribution of atmospheric precipitation, a significant moisture deficit and frequent strong winds blowing at different times of the year [9].

The relief of the Tokrau River valley basin is relatively flat and less rugged compared to the northern mountainous part of the region.

Specifically, the valley of the Tokrau River widens significantly in this section. Over a stretch of 120 kilometers along its course, the Tokrau River valley receives only two intermittent tributaries, namely, the Kusak from the left and the Zhilanshchik-Espe from the right. These intermittent streams merge with the main valley approximately near the settlement of Duvanshi, about 35–40 kilometers downstream of Ak-Tumsuk. In terms of the overall river feeding, the Kusak and Zhilanshchik-Espe intermittent streams play a relatively minor role, as their catchment areas are located at lower elevations than the main watershed.

In the Middle Tokrau deposit area, the Tokrau River valley appears as an extensive depression, ranging in width from 10 to 15–16 kilometers, with gentle, eroded, and loosely defined slopes. Further downstream, the Tokrau River valley narrows to 2–3 kilometers, forming the Karatal gorge, and continues in this manner for about 25–30 kilometers to the Cholak gorge, where it widens again to 6–8 kilometers. A distinctive feature of the southern section is the clearer contours of the cross-sectional profile of the valley, which bears signs of asymmetry due to the steeper left slope, primarily composed of granites. The morphological features of the valley floor throughout the entire deposit area are generally uniform. It appears as a flat plain with a desert–steppe landscape, covered with wormwood and low-lying bushes of boialych. In places where groundwater emerges, moisture-loving vegetation such as reeds and tamarisk thrives. Along the riverbed, there are occasional thickets of tamarisk and poplar. To the east, in the marginal part of the valley, there is a relatively extensive saucer-shaped depression called Sor-Tuz, filled with a wet salt flat. The flat surface of the valley floor is only slightly interrupted by the river channel and rocky hillocks.

In addition to the main riverbed, through which spring floodwaters flow, the valley floor is marked by numerous old riverbeds and depressions. The lower section of the valley basin, from the Cholak gorge to Lake Balkhash, forms an extensive delta with a flat surface bounded by gentle slopes. As it approaches Lake Balkhash, the main banks of the river sharply diverge to the west and east. The course of the Tokrau River is weakly pronounced in this area and gradually disappears approximately 12–15 kilometers downstream from the Cholak gorge. The reemerging riverbed near Lake Balkhash is small and covered with vegetation. The hydrographic network of the region primarily belongs to the Tokrau River basin. The Tokrau River is part of the Lake Balkhash basin and originates from the Kushoky, Saran, and Kyzyltas Mountains. The largest right-bank tributaries include Zhalanash, Zhilanshchik-Espe, and the left-bank tributaries include Karamendy, Kosobay, Karatal, Zhenishke, and Kusak. There is no continuous surface flow in the main Tokrau River channel. The river comes to life only for a short period during the spring floods. Spring surface flow occurs only in years of high water or those with average water levels [10–11].

Materials and methods

In recent decades, multispectral and hyperspectral remote sensing data have provided unprecedented opportunities for early mineral exploration and environmental hazard monitoring. The growing demand for mineral resources due to industrialization and the exponential population growth underscores the need to replenish exploitable reserves by exploring new potential mineral deposit areas. The identification of lithology in host rocks, geological structure characteristics and mineral zones of hydrothermal alterations is the most prominent application of multispectral and hyperspectral satellite remote sensing data in mineral exploration in metallogenic provinces and border regions worldwide [12–16]. Numerous ore deposits, such as orogenic gold, copper porphyry deposits, carbonatites, massive sulfides, epithermal gold, podiform chromites, uranium, magnetite and iron oxide copper gold (IOCG) deposits, have been successfully explored and discovered using multispectral and hyperspectral satellite imagery in remote sensing [17–21].

To address the objectives of this study, images from the LANDSAT satellite were used. The Landsat program, jointly developed by NASA and the U.S. Geological Survey (USGS), consists of a series of satellites that were first launched in 1972. Over the years, several generations of these satellites have been deployed, all equipped with advanced instruments for monitoring and collecting data on various aspects of Earth's surface. Landsat satellites gather information across various spectral ranges, enabling creation of multi-channel visual representations. These satellites provide global coverage, making the Landsat program a valuable resource for monitoring

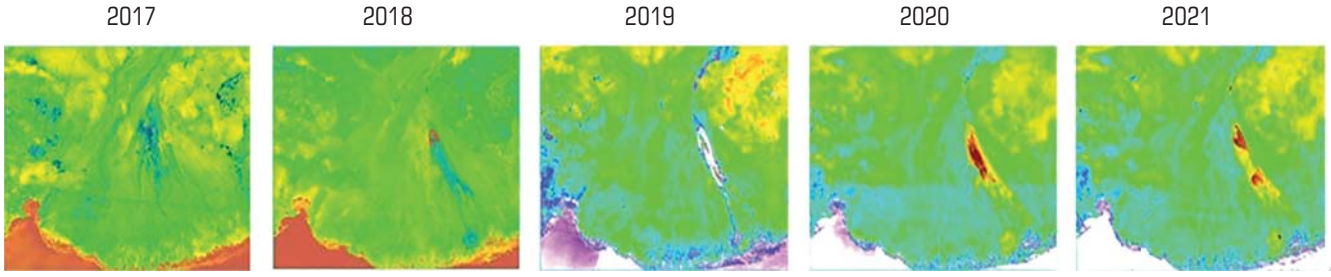

Fig. 3. Results for the Ferrous Minerals Index

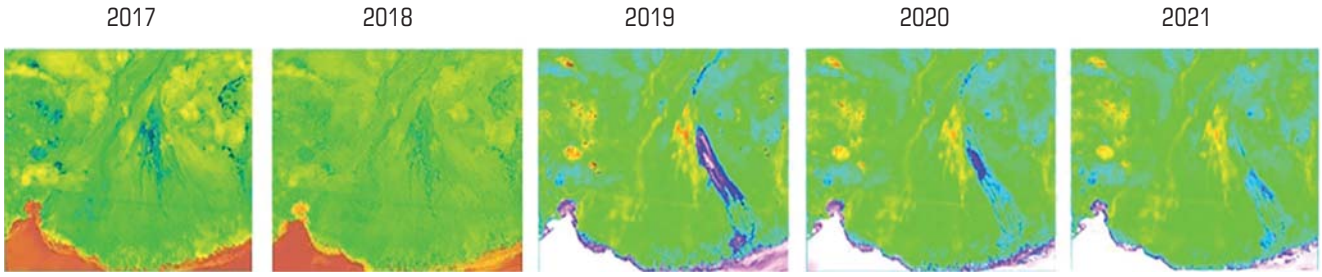

Fig. 4. Results for the Iron Oxide Index

changes occurring on our planet. It is used for both scientific and practical purposes, and there is open access to these valuable data. The data acquisition frequency is 16 days, and the image resolution is 30 meters. For this research, images from Landsat-7, 8, and 9 satellites were used [22–25].

Sentinel-2 is a space-based Earth observation system provided by the European Space Agency (ESA) as part of the Copernicus program. The Sentinel-2 satellite has a wide spectral range, covering visible, infrared and thermal wavelengths. It is equipped with 13 spectral channels, facilitating the acquisition of diverse data related to Earth's surface properties. Sentinel-2 provides a level of accuracy down to 10 meters in certain channels, making it valuable for detailed mapping and monitoring. These satellites orbit the Earth at an interval of approximately 5 days [26].

The Clay Minerals Index, abbreviated as CM, is used to identify objects with mineral constituents that include alunite and clays. Utilizing two spectral channels in the SWIR (Short-Wave Infrared) region, the results of this index are applied in collaboration with other geological indices. It is calculated using formula (1) [27]:

$$CM = \frac{SWIR1}{SWIR2} \quad (1)$$

The processed results based on this geological index are presented in **Fig. 2.**

Many types of ore exhibit relatively high reflectance values in the center of the fifth spectral channel (NIR). However, clay minerals such as montmorillonite, kaolinite and others contain an absorption feature at around 2.2 micrometers in the center of the seventh spectral channel (SWIR). The studied clay mineral index operates on the premise that clay minerals, including those with high water content, absorb within the 2–2.3 micrometer range. As a result, the processed areas exhibit minimal changes in illumination, which are related to the terrain relief [28].

The Ferrous Minerals Index, abbreviated as FM, is one of the geological indices used to detect areas with iron-bearing mineral concentrations, often associated with ore deposits. This index utilizes the SWIR-1 and NIR spectral channels during processing. Like any geological index, the results of ferrous minerals are typically applied in combination with other indices [29]. It is calculated using formula (2):

$$IO = \frac{RED}{BLUE} \quad (2)$$

Using raster calculator software, the satellite images were processed for the area of interest, and the results are presented in **Fig. 3**.

The Iron Oxide Index is a correspondence between the wavelengths of red and blue light. Due to the presence of limonite, which contains biotite and changing oxides of lake minerals, we can observe how these changes are absorbed by the blue channel, resulting in the reflectance of the red channel. Together, this index highlights areas with concentrated iron content, making them appear brighter in the processed image (**Fig. 4**). In other words, the characteristic of the studied index processes the image in a way that dampens differences in the illumination of the terrain that arise due to shading [30]. It is calculated using formula (3).

$$Ferrous\ Minerals\ Ratio = SWIR / NIR \quad (3)$$

Both Landsat and Sentinel-2A satellite images were processed. However, since Sentinel-2A satellite data were limited to the period from 2017 to 2021, the decision was made to conduct the analysis based on the data obtained from the processing of Landsat satellite images.

Results and discussion

Satellite images can be used not only for visualizing data in a familiar realistic format but also for the analysis and processing of information contained within these data. Using ArcGIS software and its data processing tools, images from various sources and different time intervals can be used to analyze the concentration, distribution, location, changes in vegetation, mineral, and water resources in the study area. The calculated geological indices shown in **Fig. 5** provide the opportunity to determine the enrichment of land areas with valuable minerals. Figure 5 shows the areas of the Konyrat deposit, where mineral concentration can be observed using processed images from the year 2009.

The analysis of satellite images of the Tokrau River delta area visualizes the widespread occurrence of fluffy simple solonchaks as well as takyr — constant companions of the semi-desert arid climate — within the edge part of the valley's bottom, especially in the river's lower flow. To the east, in the valley's edge part, there are stretches a fairly extensive bowl-shaped depression of Sor Bektay, filled with wet solonchak. **Figure 6**, with regard to the areas marked with the number 1, which correspond to Sor Bektay, demonstrates favorable conditions for the natural synthesis of iron oxide, namely, magnetite, in the moist solonchaks of this area. This is

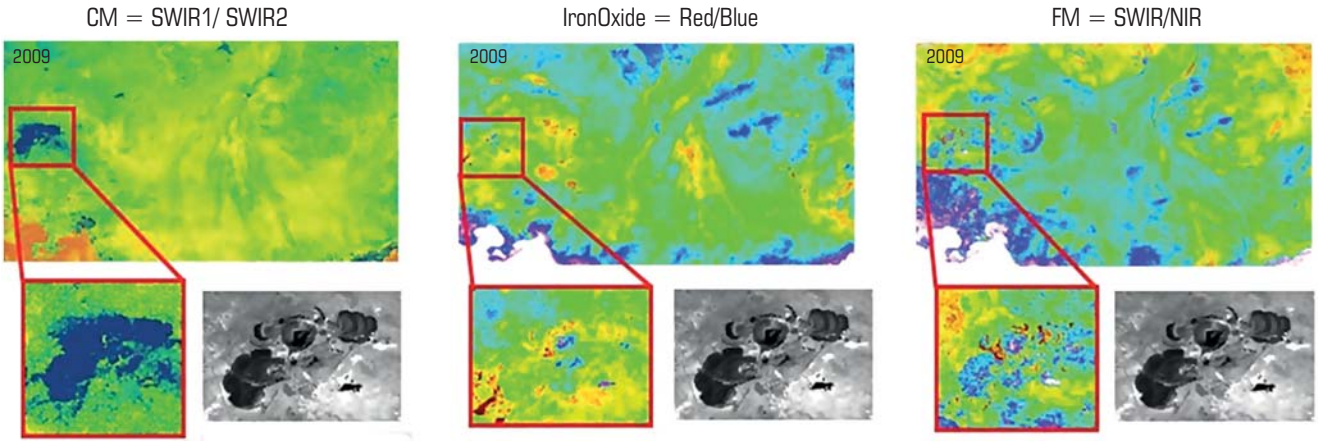

Fig. 5. Mineral concentration at the Konyrat deposit

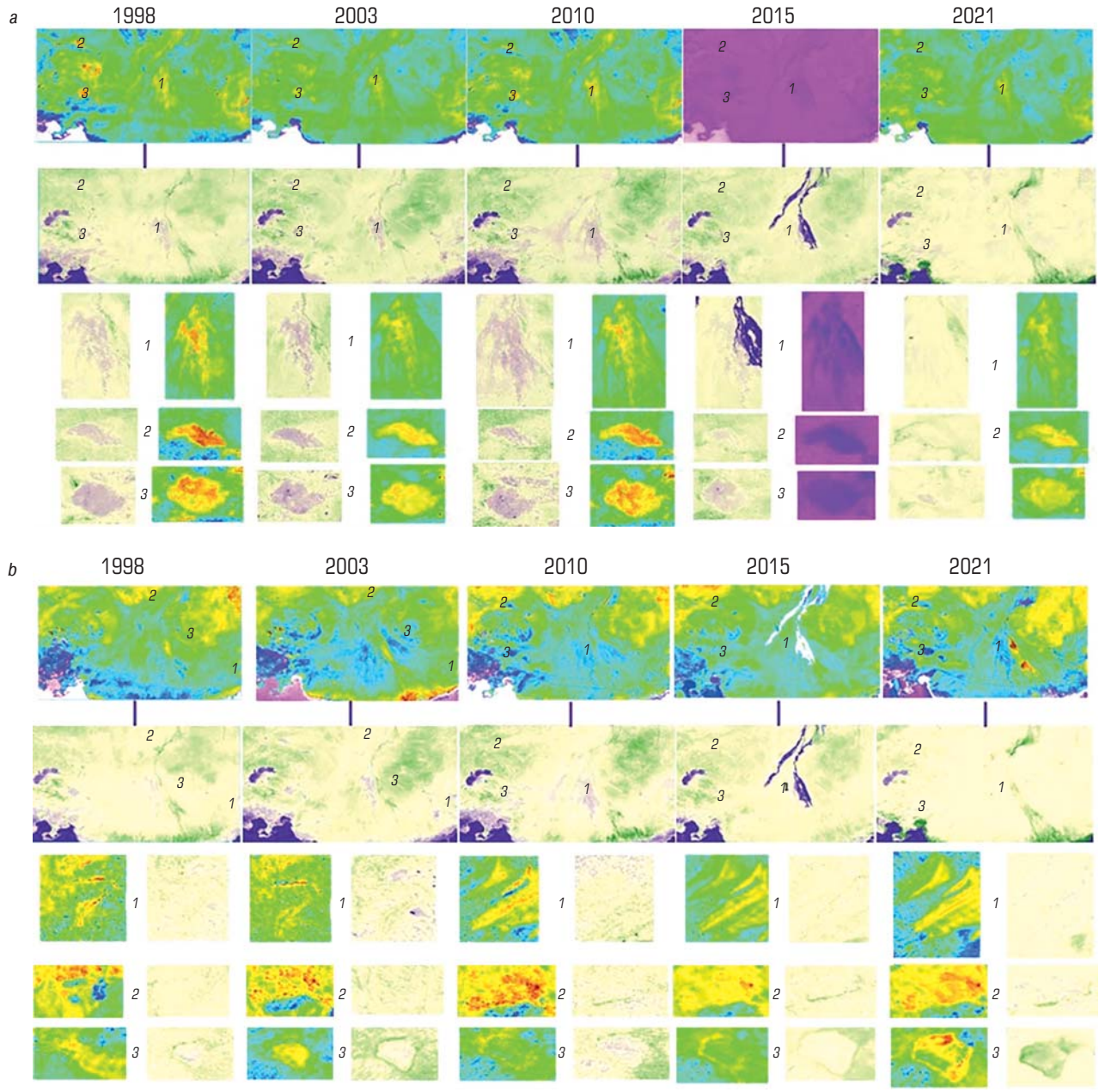

Fig. 6. Analysis of processed images using the Iron Oxide Index (*a*) and Ferrous Minerals Index (*b*)

substantiated by the changes visible on the processed images, indicating an increased concentration of magnetite in the specified zone. The slightly alkaline environment, characteristic of the moist solonchaks of Sor Bektay, facilitates formation of magnetite, as confirmed by the analysis of remote sensing data [31].

The above-presented analysis proves the indirect estimates obtained using the NDVI vegetation index. The vegetation index best highlights the importance of comparing data on the condition of vegetation in different time periods. In order to demonstrate the accuracy of the obtained results using the geological indices in comparison with the vegetation index, three different areas with the highest mineral concentrations were selected for the analysis for each index. The clay minerals index revealed that after spring floods, the riverbed begins to be covered with healthy vegetation, and in these same locations, there are vividly expressed areas with a concentration of clay minerals. This leads to the conclusion that in places with healthy vegetation, there is a predominance of clay levels, which subsequently affects plant health. However, in places where healthy vegetation was observed in 1998, by 2021 such conditions are no longer observed, indicating changes in the mineral composition and/or plant growth conditions. Additionally, for accuracy of results and georeferencing, GNSS technologies can be utilized [32, 33].

It was revealed that in areas with mineral concentration, the level of vegetation decreases. In places indicated by numbers 2 and 3, there are areas with high mineral concentration, which also indirectly demonstrates the presence of iron oxide concentration through the vegetation index, as areas with magnetite concentration show no development of healthy vegetation. It is clearly seen in the images that the highlighted areas are characterized by patches of milky soil. It is also worth noticing that concentration of magnetite decreases over time, and comparing the results of 1998 and 2021, a decrease in iron oxide and an increase in healthy vegetation can be observed.

Conclusions

Satellite images offer numerous advantages, especially in the context of tracking changes over time, such as changes in coastlines, island enlargement and deforestation. These images can back up additional investigations and possibly provide supporting evidence. Based on the analysis of the data, the following conclusions can be drawn. Landsat-8 satellite is preferable for studying large areas on Earth due to its spatial resolution, while Sentinel-2A is a versatile method due to higher spatial resolution and more frequent imaging, allowing it to cover wide areas with low frequency and high detail.

Processing the Clay Minerals, Ferrous Minerals and Iron Oxide indices in the study area, it can be concluded that there is no significant accumulation of minerals near the Tokrau River compared to the Konyrat deposit, while about 10–11 km to the north of the river, there are small areas with similar readings as in the Konyrat area.

Clay minerals are frequently found in areas with widespread healthy vegetation. However, over time, due to a decrease in the concentration of clay minerals, the overall condition of vegetation deteriorates. Specifically, plants wither.

In areas dominated by healthy vegetation, a decrease in magnetite concentration and an increase in clay mineral concentration can be noticed. In areas where there was a concentration of clay minerals and vegetation was damaged, an increase in magnetite concentration and a decrease in all others are observed.

Acknowledgments

The research is funded by the Committee of Science of the Ministry of Science and Higher Education of the Republic of Kazakhstan (Grant No. BR21882179).

References

1. Baugh W. M., Kruse F. A., Atkinson Jr. W. W. Quantitative Geochemical Mapping of Ammonium Minerals in the Southern Cedar Mountains, Nevada, Using the Airborne Visible/Infrared Imaging Spectrometer (AVIRIS). *Remote Sensing of Environment*. 1998. Vol. 65, No. 3. pp. 292–308.
2. Abrams M. J., Brown D. Silver Bell, Arizona, porphyry copper test site. *The Joint NASA — Geosat test case study, Section 4. American Association of Petroleum Geologists*. 1985. 73 p.
3. Sabins F. F. Remote sensing for mineral exploration. *Ore Geology Reviews*. 1999. Vol. 14, Iss. 3–4. pp. 157–183.
4. Spatz D. M., Wilson R. T. Exploration remote sensing for porphyry copper deposits, western America Cordillera. *Proceedings of the Tenth Thematic Conference on Geologic Remote Sensing. Environmental Research Institute of Michigan*. 1994. pp. 1227–1240.
5. Sabins F. F. Remote sensing — Principles and interpretation, 3rd ed. New York : W. H. Freeman and Co., 1997. 494 p.
6. Watson K., Kruse F. A., Hummer-Miller S. Thermal infrared exploration in the Carlin trend, northern Nevada. *Geophysics*. 1990. Vol. 55. pp. 70–79.
7. Bennett S. A., Atkinson W. W., Kruse F. A. Use of thematic mapper imagery to identify mineralization in the Santa Teresa District, Sonora, Mexico. *International Geology Review*. 1993. Vol. 35, Iss. 11. pp. 1009–1029.
8. Zhang X., Pazner M., Duke N. Lithologic and mineral information extraction for gold exploration using ASTER data in the south Chocolate Mountains (California). *ISPRS Journal of Photogrammetry and Remote Sensing*. 2007. Vol. 62, Iss. 4. pp. 271–282.
9. Baibatsha A. B., Mamanov E. Zh. Geology and geodynamics of Karsakpay–Ulytau geostuture zone and its prospects for minerals. *News of the Academy of Sciences of the Republic of Kazakhstan. Series of Geology and Technical Sciences*. 2017. Vol. 1, No. 421. pp. 46–62.
10. Baibatsha A. B., Omarova G., Dyussembayeva K. Sh., Kassenova A. T. Kokkiya — A promising for Kazakhstan gold-metasomatic type of deposit. *16th International Multidisciplinary Scientific Geoconference — SGEM 2016*. 2016. Vol. 1. 2016. pp. 289–296.
11. Baibatsha A. B., Bekbotaeva A. A., Bekbotayev A. T. Ore minerals of Carboniferous copper sediment-hosted Zhezkazgan deposit (Central Kazakhstan). *Proceedings of the 15th International Multidisciplinary Scientific GeoConference — SGEM 2015*. 2015. pp. 329–337.
12. Stasiv I. V. On the origin of lake Balkhash and Balkhash — Alakol depression. 2020. *Sci-Article.ru*. No. 78. pp. 11–20.
13. Egizkoitas. Kazakhstan. National Encyclopedia. Almaty : Kazak entsiklopediyasy, 2005. Vol. II.
14. The Great Soviet Encyclopedia. Prohorov A. M. 3rd edition. Moscow : Sovetskaya entsiklopedia, Vol. 30. 1978. 631 p.
15. Mars J. C., Rowan L. C. Spectral assessment of new ASTER SWIR surface reflectance data products for spectroscopic mapping of rocks and minerals. *Remote Sensing of Environment*. 2010. Vol. 114, Iss. 9. pp. 2011–2025.
16. Pour B. A., Hashim M. The application of ASTER remote sensing data to porphyry copper and epithermal gold deposits. *Ore Geology Reviews*. 2012. Vol. 44, pp. 1–9.
17. Noori L., Pour B. A., Askari G. et al. Comparison of different algorithms to map hydrothermal alteration zones using aster remote sensing data for polymetallic vein-type ore exploration: Toroud–Chahshirin Magmatic Belt (TCMB), North Iran. *Remote Sensing*. 2019. Vol. 11, Iss. 5. ID 495.
18. Ninomiya, Y., Fu B. Thermal infrared multispectral remote sensing of lithology and mineralogy based on spectral properties of materials. *Ore Geology Reviews*. 2019. Vol. 108. pp. 54–72.
19. Pour A. B., Park Y., Park T. S. et al. Regional geology mapping using satellite-based remote sensing approach in Northern Victoria Land, Antarctica. *Polar Science*. 2018. Vol. 16. pp. 23–46.
20. Bolouki, S. M., Ramazi H. R., Maghsoudi A., Pour A. B., Sohrabi G. A Remote sensing-based application of Bayesian networks for epithermal gold potential mapping in Ahar-Arasbaran Area, NW Iran. *Remote Sensing*. 2020. Vol. 12, Iss. 1. ID 105.
21. Sekandari M., Masoumi I., Pour A. B. et al. Application of Landsat-8, Sentinel-2, ASTER and WorldView-3 spectral imagery for exploration of carbonate-hosted Pb-Zn deposits in the Central Iranian Terrane (CIT). *Remote Sensing*. 2020. Vol. 12, Iss. 8. ID 1239.

22. Mars J. C., Rowan L. C. Regional mapping of phyllic-and argillic-altered rocks in the Zagros magmatic arc, Iran, using Advanced Spaceborne Thermal Emission and Reflection Radiometer (ASTER) data and logical operator algorithms. *Geosphere*. 2006. Vol. 2(3). pp. 161–186.
23. Available at: https://www.usgs.gov/landsat-missions/landsat-satellite-missions (Accessed: 04.04.2024).
24. Duuring P., Hagemann S. G., Novikova Y., Cudahy T., Laukamp C. Targeting iron ore in banded iron formations using ASTER data: Weld Range Greenstone Belt, Yilgarn Craton, Western Australia. *Economic Geology*. 2012. Vol. 107. pp. 585–597.
25. Ducart D. F., Silva A. M.; Toledo B., Assis L. Mapping iron oxides with Landsat-8/OLI and EO-1/Hyperion imagery from the Serra Norte iron deposits in the Carajás Mineral Province, Brazil. *Brazilian Journal of Geology*. 2016. Vol. 46. pp. 331–349.
26. Available at: https://sentinel.esa.int/web/sentinel/missions/sentinel-2 (Accessed: 04.04.2024).
27. Dogan H. M. Mineral composite assessment of Kelkit River Basin in Turkey by means of remote sensing. *Journal of Earth System Science*. 2009. Vol. 118. pp. 701–710.
28. Bergaya F., Theng B.K.G., Lagaly G. Developments in Clay Science Series. Handbook of Clay Science. Amsterdam : Elsevier, 2006. 1224 p.
29. ArcGIS. Channel Indexes. Available at: https://pro.arcgis.com/ru/pro-app/latest/arcpy/spatial-analyst/bai.html (Accessed: 04.04.2024).
30. Segal D. B. Theoretical basis for differentiation of ferric-iron bearing minerals, using Landsat MSS Data. *Proceedings of Symposium for Remote Sensing of Environment, 2nd Thematic Conference on Remote Sensing for Exploratory Geology, Fort Worth, TX*. 1982. pp. 949–951.
31. Rockwell B. W., Gnesda W. R., Hofstra A. H. Improved automated identification and mapping of iron sulfate minerals, other mineral groups, and vegetation using Landsat 8 Operational Land Imager Data, San Juan Mountains, Colorado, and Four Corners Region. *US Geological Survey*. 2021. No. 3466. DOI: 10.3133/sim3466
32. Orynbassarova E, Yerzhankyzy A, Shults R, Roberts K, Togaibekov A. Strategies of GNSS processing and measuring under various operational conditions. *Naukovyi Visnyk Natsionalnoho Hirnychoho Universytetu*. 2022. No. 3. pp. 146–150.
33. Akhmetov R., Makhmetova G., Orynbassarova E., Baltiyeva A., Togaibekov A. et al. The study of kinematic GNSS surveying for BIM georeferencing. *The International Archives of the Photogrammetry, Remote Sensing and Spatial Information Sciences*. 2022. Vol. XLVI-5/W1-2022. pp. 7–14. EM